Computation of Vortex Flow Around a Canard/Delta Combination

Lars-Erik Eriksson* and Arthur Rizzi†
FFA, The Aeronautical Research Institute of Sweden, Bromma, Sweden

The inviscid compressible and rotational flow around an isolated 55 deg swept sharp edged delta wing, and around that same wing closely coupled with a canard, is computed at transonic speeds by using meshes of O O type around the main wing, constructed by transfinite interpolation, and by using a time marching finite volume procedure to obtain steady state solutions to the Euler equations The canard is represented as a slit in the mesh Results of these computations, performed on a CYBER 205 vector processor, show that the flow model predicts leading edge vortex separation on the main wing, and in the wing-alone case the overall flow agrees qualitatively with that deduced from oil flow pictures for a similar wing In the canard/delta case, the deflection of the flow due to the canard is verified by velocity vector plots, and the influence on the wing pressure distribution is found to be realistic Cross flow velocity plots show that the canard creates a vortex of its own which interacts with the flow over the main wing

Introduction

FLOWS with shed vorticity are important in aerodynamics, especially for wings of large sweep and small aspect ratio The characteristic feature of such flows is the generation of vorticity at the edges of the wing and the subsequent con vection of this vorticity along streamlines Except for the actual generation of vorticity, which is a very local phenomenon, involving irreversible thermodynamic processes and an entropy production, these flows are effectively in viscid Recently, it has been found that the Euler equations admit solutions for these types of flows which has generated much excitement in computational fluid dynamics because this flow model allows vortex sheets to be captured automatically in the solution Previous flow models based on potential theory require them to be hand fitted, which is a cumbersome and difficult process, especially for multiple lifting surfaces

Although the vortex generating mechanism in the Euler equation model is still much debated, a number of solutions to the discretized equations have been presented[1-6] with vorticity being shed from the leading edge of a highly swept 70 deg delta wing, the so-called Dillner wing These speak for a mechanism in at least the discrete model for generating vorticity The authors, however, do not investigate this mechanism in further detail here, nor do they attempt to justify their computational procedure by showing the degree of accuracy of the resolved vortex over this standard delta wing case. Such a detailed inspection would turn into a full-length paper of its own Readers interested in such a thorough discussion and an up to date comparison of computed results for leading edge vortex flow shed from a 70-deg delta ob tained from the currently best known methods (the authors' included) are referred to the forthcoming report of AGARD Working Group 07 [7] The purpose of this paper is to explore further how the vortex-sheet capturing ability of the Euler equation model may depend on wing sweep angle and con figuration complexity Two calculations for a delta wing at intermediate sweep angle are presented The first is an isolated delta wing of 55 deg sweep, and the second is that same delta wing closely coupled with a canard ahead of it To the best of the authors' knowledge, this latter computation is the first of its kind Although the absolute accuracy of these two solutions remains to be calibrated, they can be used together to show the relative effect of the canard For practical use this may be all that is needed.

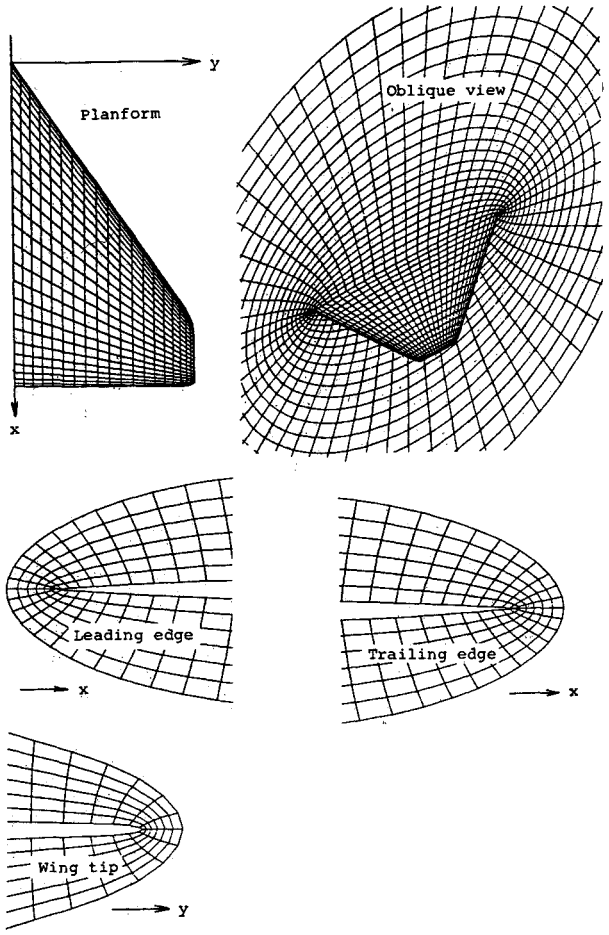

Fig 1 Standard O O mesh for single delta wing with 55 deg leading edge sweep.

Received Jan 17 1984; revision received June 1, 1984

*Research Scientist Aerodynamics Department
†Research Scientist Aerodynamics Department Member AIAA

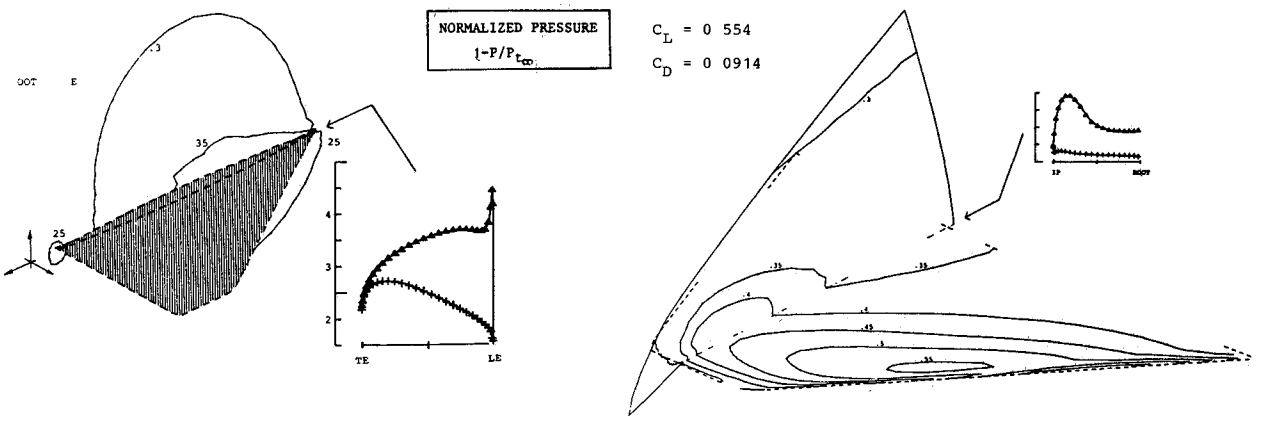

a) Isobars of normalized pressure, $1-p/p_{t\infty}$.

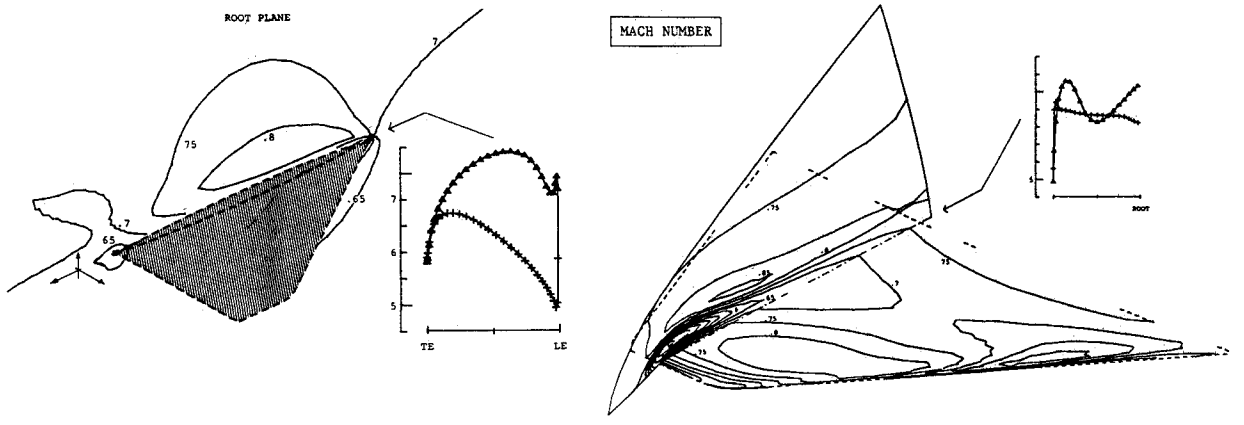

b) Lines of constant Mach number

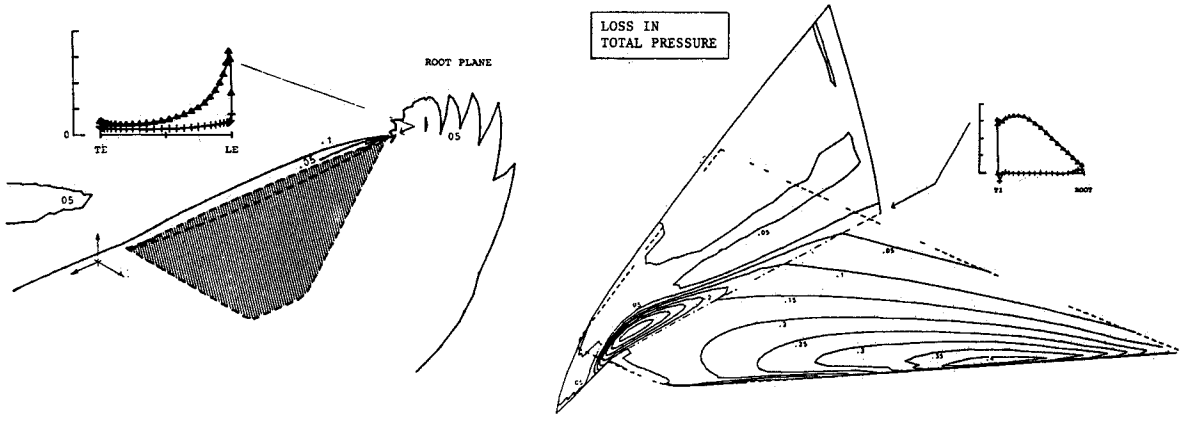

c) Contours of constant total pressure loss, $1-p_t/p_{t\infty}$

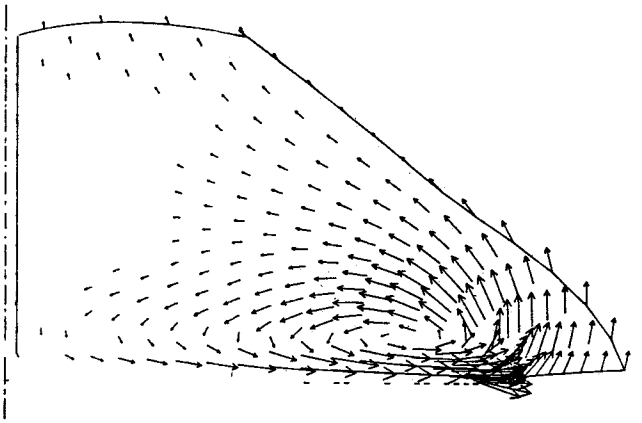

d) v w velocity vector plot in the 67 5% constant chord surface

Fig 2 Flow properties computed in the root plane and on and above the upper surface of the cropped sharp edged 55 deg swept delta wing for $M_\infty = 0$ 70 and $\alpha = 10$ deg The flowfield is surveyed by isograms in the root plane, on the upper surface, and in an intersecting mesh surface extending outward from the 67.5% chord station of the wing Along the intersection lines of the wing in the root plane and the wing with the 67 5% chord station the flow properties on the upper and lower surface are plotted vs the local chord and span direction, respectively The displayed properties are as shown in Figs 2a f

(Figure continued on next page)

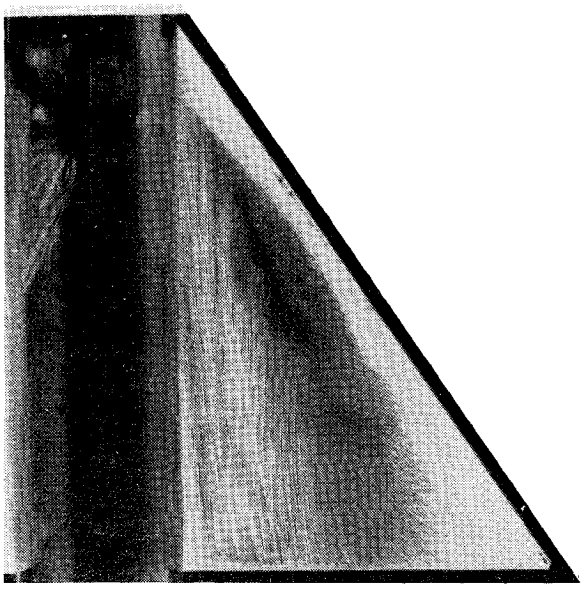

e) Oil flow picture for a similar 55 deg swept delta wing at Mach 0 80 and 10 deg angle of attack displays nonconical flow in the apex region.

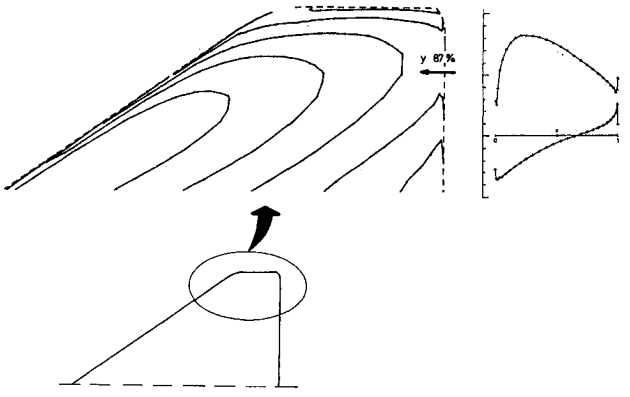

f) Detail of isobar pattern on upper surface of single delta wing showing local disturbance at the trailing edge underneath the main vortex Chordwise pressure distribution at 87% span station shows the local trailing edge loading in this region

Outline of Numerical Method

The authors' method[4] of generating three dimensional meshes around wings is based on the concept of transfinite interpolation and gives the desired mesh coordinates in the interior of the flowfield by interpolating among the given boundary meshes Normal derivatives of the coordinates at the boundaries are used where needed to control the mesh at these surfaces A novel feature of the method is that it has been generalized to handle slits in the computational domain, which makes it possible to insert additional lifting surfaces in the vicinity of the main wing

The authors' method[2] of solving for three-dimensional vortex flowfields is a time dependent finite volume approach that uses a multistage explicit time integration scheme together with centered space differences to solve the compressible Euler equations Significant features of this approach are its integral conservation law form important for the correct capturing of shock waves and vortex sheets, its amenability to very general geometry without the need for a global coordinate transformation, and its tolerance of mesh singularities because the flow equations are balanced only within the cells of the grid [3] and not at the nodal points

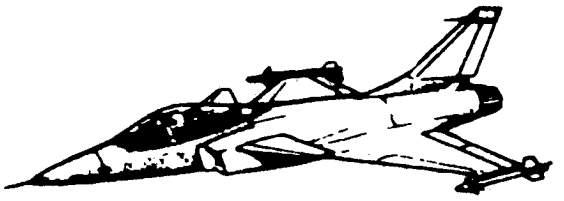

Fig 3 Modern combat aircraft with canard/delta wing combination

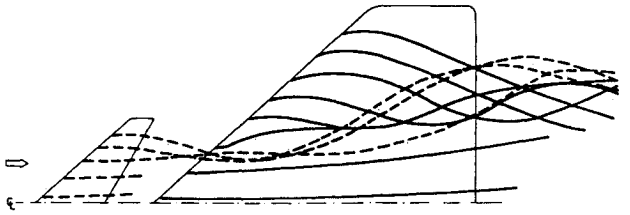

Fig 4 Influence of a closely coupled canard over the flow of the main wing

Single Delta Wing

Mesh Generation

The first case presented is a cropped delta wing with a leading edge sweep of 55 deg and zero trailing edge sweep A simple 4% thick parabolic arc profile defines all chordwise sections of the wing and no camber or twist has been added The mesh used for this wing (Fig 1) is the standard O O type mesh previously used for ordinary quadrilateral wings and, thus, is not the special delta wing type mesh presented previously [1] There are two reasons for this choice: 1) the moderate leading edge sweep does not particularly favor any one of the two mesh alternatives when considering mesh density or mesh skewness around the main wing and 2) the standard O O mesh is better suited for modeling the canard in the form of a slit The overall mesh dimensions used for the flow computations are: 56 cells around the chord 20 in the spanwise direction, and 32 in the outward direction

Results

The results of the flow computations for the single delta wing at a freestream Mach number of 0 70 and 10 deg angle of attack reveal a number of interesting features in this flow As the pressure, Mach number, and total pressure contours on the upper surface clearly indicate (Figs 2a c) leading edge vortex separation is obtained, but seems to start some distance downstream of the wing apex This behavior differs from that obtained at higher sweep angles, in which case separation starts immediately at the apex [1] It is as yet unclear whether this difference is caused by the artificial viscosity in the flow model or by the physics of inviscid flow Experimental results[5] in the form of oil flow pictures for a similar wing at the same freestream Mach number show that for a certain incidence range, leading edge separation does in fact start downstream of the apex (see Fig 2e) In view of this, the computed flow pattern appears to be quite realistic We remark further that the vortex dominates our flowfield much more than it does the corresponding one computed by a singularity method for conical flow [8]

Another interesting feature of the computed flow is the appearance of a very local trailing edge loading just where the main vortex passes over the trailing edge (Fig 2f) Again there are two possible explanations for this phenomenon, one physical and one numerical Either it is caused by an interaction between the main vortex and the vortex sheet emitted at the trailing edge or else it is a purely numerical effect due to the sharp trailing edge However the fact that

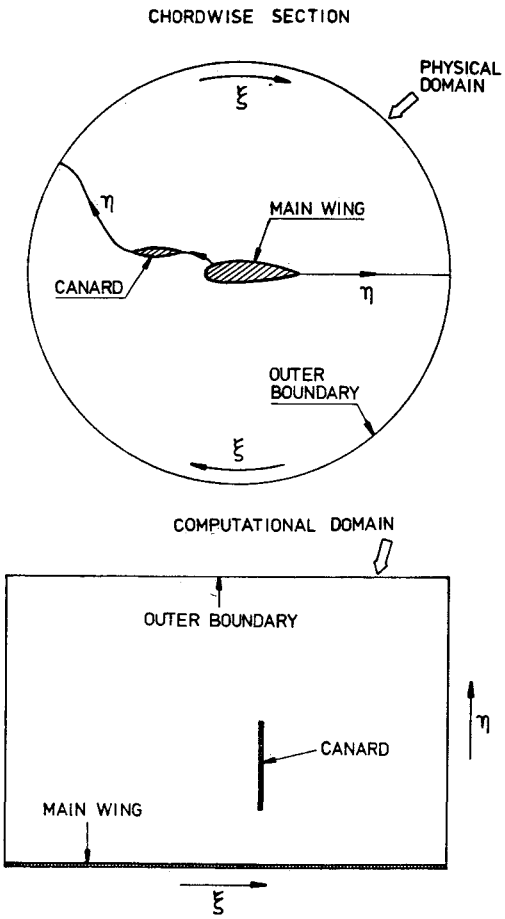

Fig 5a Mesh topology in the root plane for the canard/delta combination The canard is represented by a double valued slit in the computational domain

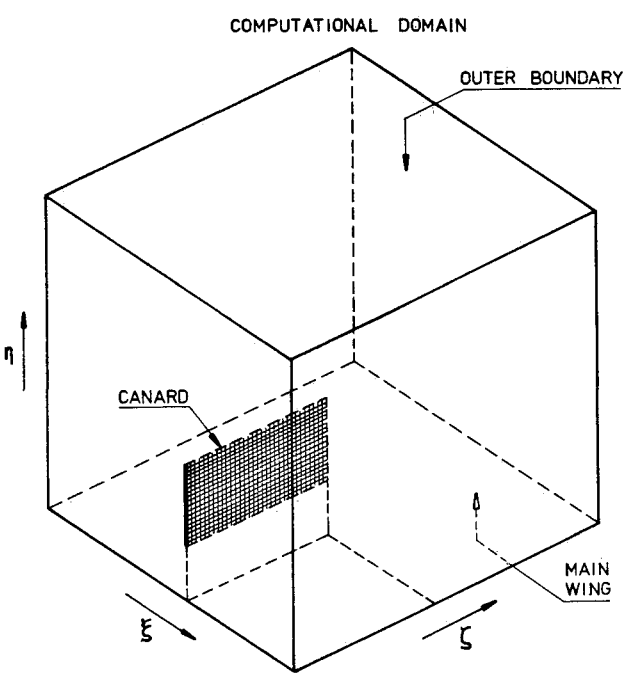

Fig 5b Overall mesh topology for the canard/delta combination The canard is represented by a double-valued slit surface in the computational domain where solid wall boundary conditions are applied

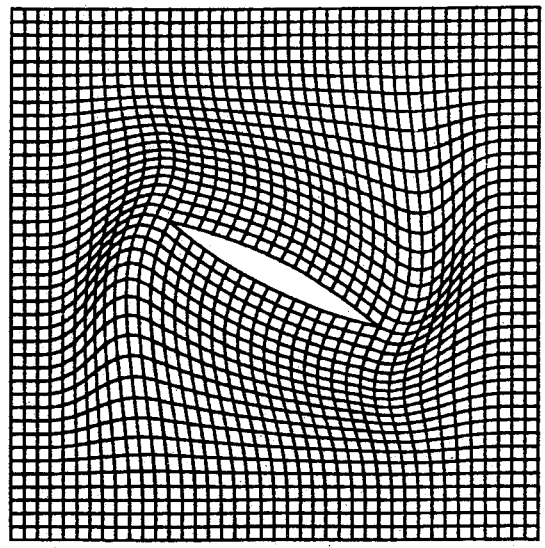

Fig 6 Two dimensional demonstration of the transfinite interpolation technique extended to slits A Cartesian mesh is deformed to conform to a circular arc profile with full control of the direction and spacing of the out of surface coordinate lines

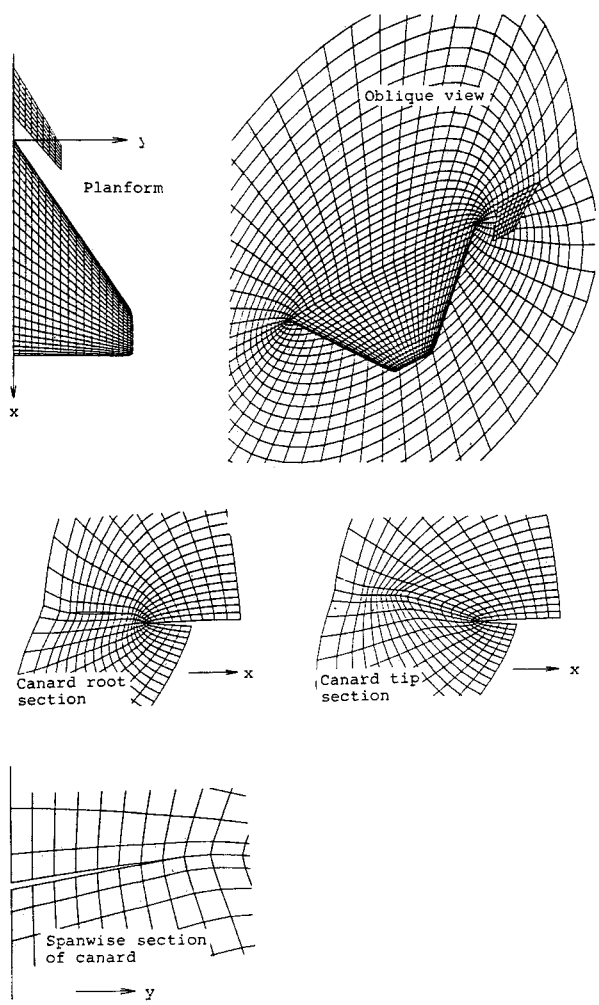

Fig 7 O O mesh for canard/delta combination Main wing is the same as that in Fig 1

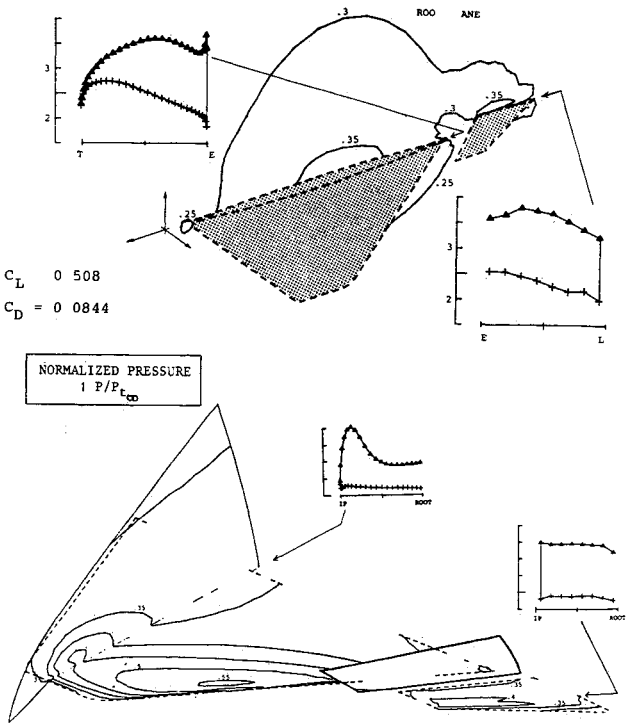

a) Isobars of $1-p/p_{t\infty}$

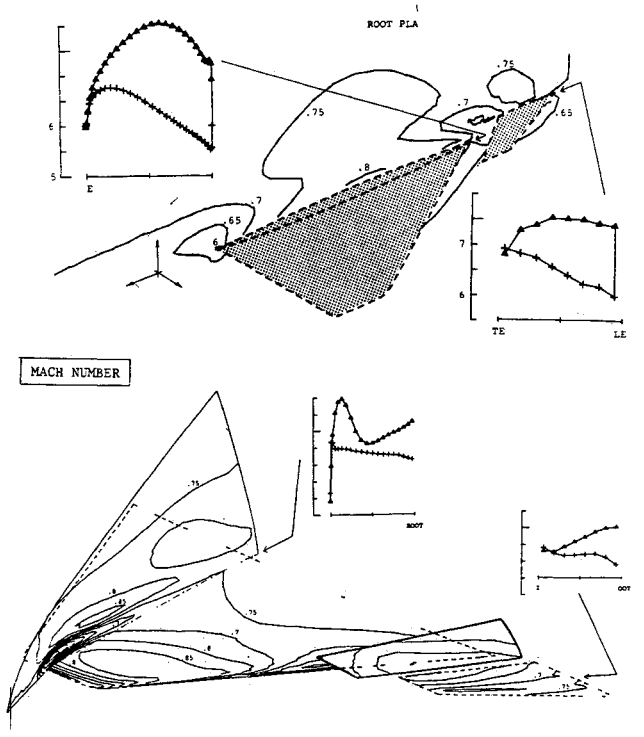

b) Lines of constant Mach number

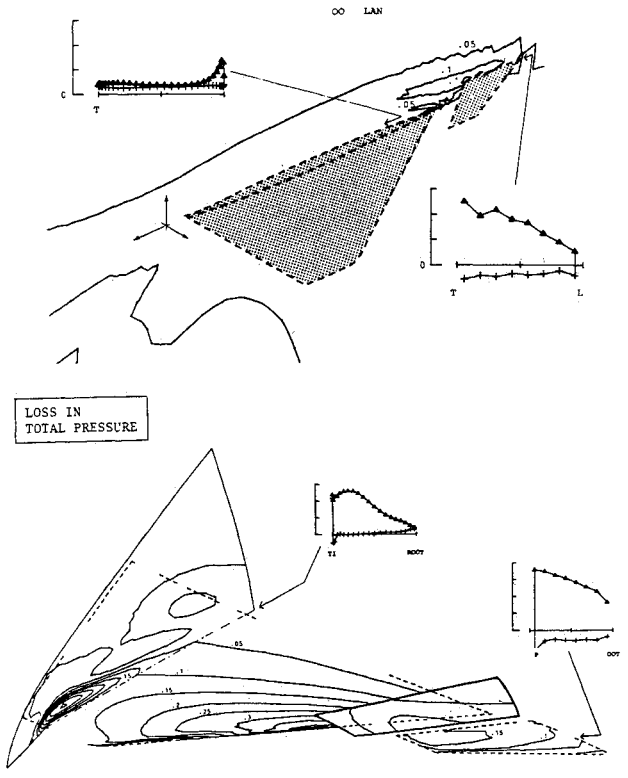

c) Contours of constant loss in total pressure, $1-p_t/p_{t\infty}$

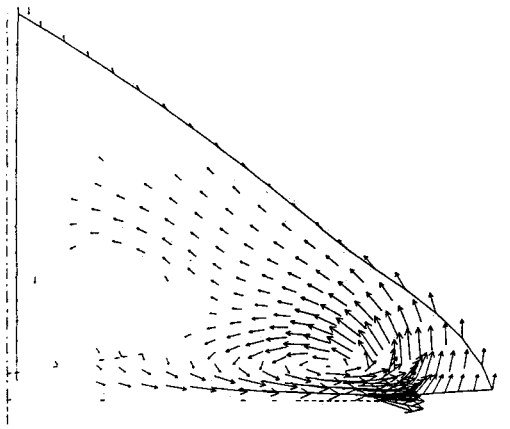

d) v w velocity vector plot in the 67 5% constant chord surface of the delta wing

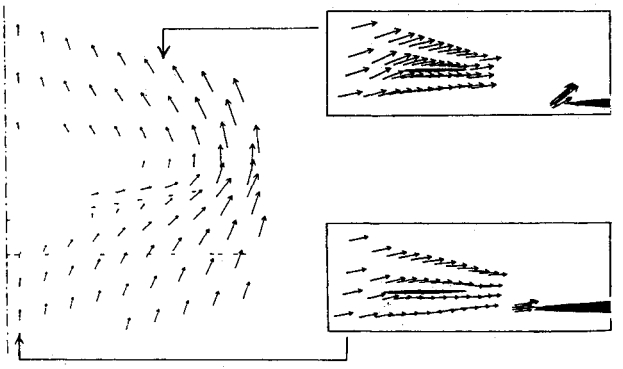

e) v w velocity vector plot (to the left) in the mesh surface that intersects the 80% constant chord station of the canard, together with u w velocity vector plots (to the right) in the root plane and in the mesh surface that intersects the 80% span station of the canard

Fig 8 Flow properties computed in the root plane and on and above the upper surface of the cropped sharp edged 55 deg swept delta wing with close coupled canard for $M_\infty = 0\ 70$ and $\alpha = 10$ deg The flowfield is surveyed by isograms in the root plane, on the upper surface of the wing and canard, in an intersecting mesh surface extending outward from the 67 5% chord station of the wing, and in a mesh surface just behind and extending above the canard Along the intersection lines of the wing and canard with the root plane, the wing with the 67 5% chord surface, and the canard with its 44% chord station, the flow properties on the upper and lower surface are plotted vs the local chord and span direction, respectively The displayed properties are as shown in Figs 8a d

such phenomena are not encountered at the trailing edge of ordinary wings with attached flow indicates that it may well reflect a real flow mechanism, though admittedly in an im perfect manner due to the coarseness of the mesh

As a striking demonstration of the ability of the Euler model to simulate vortical flows, the cross flow pattern on the upper side of the wing is shown in Fig 2d The location of the vortex in the computed flow agrees qualitatively with that deduced from the oil flow pictures in the experimental work mentioned above and even though the planforms are not quite identical the computed ($C_L = 0\ 554$, $C_D = 0\ 0914$) and measured ($C_L = 0\ 53$) lift coefficients are in good agreement

Canard/Delta Combination

If a computational method is to be useful for aircraft design it must be able to treat geometries more complicated than a single delta wing A typical modern fighter is sketched in Fig 3, and it is shown that the most simplified con figuration that still possesses the fundamental aerodynamic character of the complete plane is a closely coupled nose wing/delta wing combination whose shed vortices interact with each other (see Fig 4) Our solution method is com pletely general so that once a mesh is constructed around a canard/delta combination such as this, no modification other than the added boundary conditions of zero flow through the second wing surface needs to be implemented The mesh generation for such a geometry, however, is not a trivial matter, as will be evident from the following description

Mesh Generation

The mesh chosen for the canard/delta combination is a standard O O mesh around the main wing supplied with a slit to represent the canard (see Fig 5) This mesh topology leads to an H H type mesh around the canard, which for reasonable overall mesh dimensions cannot resolve the details of the flow there However, our primary objective is to obtain the flow deflection effect of the canard on the main wing, and for this purpose the mesh is found to be sufficiently dense

To generate this type of mesh, an extended version of the authors' transfinite interpolation method is used, which can be thought of as a two step procedure In the first step, a standard O-O mesh is generated around the main wing, and in the second step this mesh is deformed in a region around the slit so that it conforms to the canard surface The latter step, which is the novel feature here, involves the construction of a local interpolation operator for the slit and the use of this operator within the framework of transfinite interpolation Just as for the main wing, normal derivatives of the mapping function are used to control the mesh in the vicinity of the slit The details of this extended transfinite interpolation method are reported elsewhere,[9] and, therefore, will not be presented here. However, in order to demonstrate the capabilities of this technique a two dimensional example is shown (see Fig 6) where a Cartesian mesh has been deformed to conform to a circular arc profile at nonzero angle of attack

As a reasonably realistic example of a canard/delta combination, the 55 deg swept delta wing presented in the previous section was chosen as the main wing and a smaller similarly swept sharp edged wing was placed in front of it as a canard The mesh generated for this geometry (Fig 7) has the same overall dimensions as the wing alone mesh ($56 \times 32 \times 20$) and the slit is defined so that there are 8×8 cells on both the upper and lower canard surfaces

Flow Solution

As mentioned previously the basic solution method is quite general and independent of the mesh However, the in troduction of a slit in the mesh with solid wall boundary conditions certainly affects the practical coding of the method Due to the high degree of vectorization in the present code, the changes due to the slit are accomplished as local corrections after each vector statement so that the data streams are not interrupted This method works well because the number of field points that must be corrected is very small in comparison with the total number of points (see Fig 5b) For the canard/delta combination presented here the total increase in CPU time due to the canard was less than 10%

Results

The computed flow around the canard/delta combination shown in Fig 7 at a freestream Mach number of 0 70 and 10 deg angle of attack is presented in Figs 8a e Comparing these results by eye with the wing alone results in Figs 2a d, it is evident that the canard influences the flow over the main wing to a large degree The main effect on the pressure distribution is a lift reduction for the inner part of the wing and a small lift increase for the outer part of the wing As the pressure distribution on the canard shows (Fig 8a), the mesh is too coarse to resolve the details of the flow there, but the pressure difference between the upper and lower surfaces indicates that the model does simulate the flow deflection effect of the canard Further evidence of this is given by the contours of total pressure (Fig 8c) which show that the canard generates a "wake" of total pressure loss that is convected downstream over the main wing surface This indicates that the canard acts as a lifting surface that sheds vorticity into the freestream flow The final confirmation of this is given by the cross flow velocity vectors plotted in Fig. 8d, which clearly show the vortex generated by the canard

To demonstrate the effect of the canard's solid wall boundary conditions on the surrounding flow, velocity vectors around the canard are shown in Fig 8e

Comparison of Results for Single Delta and Canard/Delta Combination

As mentioned in the Introduction, the main purpose of the present study is to explore the ability of the authors' mesh generation and Euler solution methods to simulate the vortex flow around a more complex configuration such as a canard/delta combination Even though the mesh around the canard is too coarse to resolve the local details of the flow, the results presented in Figs 8a e indicate that the main flow deflection effect of the canard is obtained, which in turn means that the influence of the canard on the main wing should be fairly accurate Thus, it is likely that this type of flow simulation can be of great use in the overall wing design process The lift and drag coefficients for the single delta are $C_L = 0\ 554$ and $C_D = 0\ 0914$ When the canard is added, the coefficients for the main wing become $C_L = 0\ 508$ and $C_D = 0\ 0844$

A direct comparison between the single delta and the canard/delta combination is presented in Figs 9a-d It is evident from this comparison that the canard gives rise to a substantial lift decrease on the inner part of the wing span while it increases the lift of the outer part of the wing This behavior is quite realistic and is consistent with the notion of a vortex sheet extending downstream of the canard trailing edge which induces a "downwash" on the inner part and an "upwash" on the outer part of the main wing In Fig 9c it can also be seen that the presence of the canard increases the suction peak under the main vortex and moves it slightly toward the wing tip. The cross flow velocity vectors plotted in Fig. 9d clearly demonstrate the influence of the canard on the vortex flow above the main wing

The computational results presented in this work should of course be seen in the light of the current rapid development of supercomputers like CYBER 205, both in terms of computing speed and real memory Even at this time there exist vector processors with extended real memory which would allow us to recompute the cases in this work with twice as many grid points in the I J, and K directions With such dense meshes it is likely that some of the local details of the flow around the canard could be resolved satisfactorily

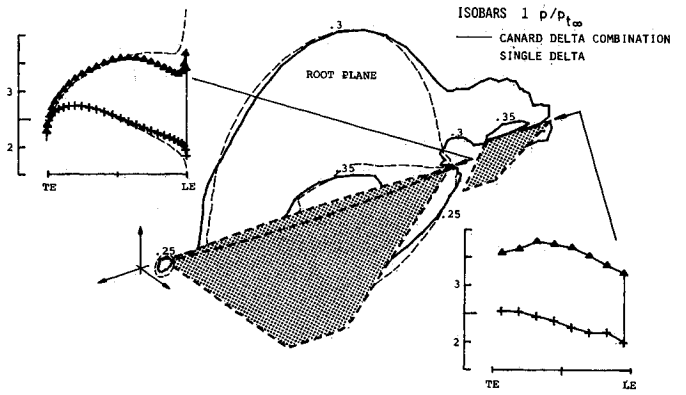

Fig 9a Influence of canard on pressure distribution (lines of constant normalized pressure $1-p/p_{t\infty}$) at the plane of symmetry The single delta case is indicated with dashed lines

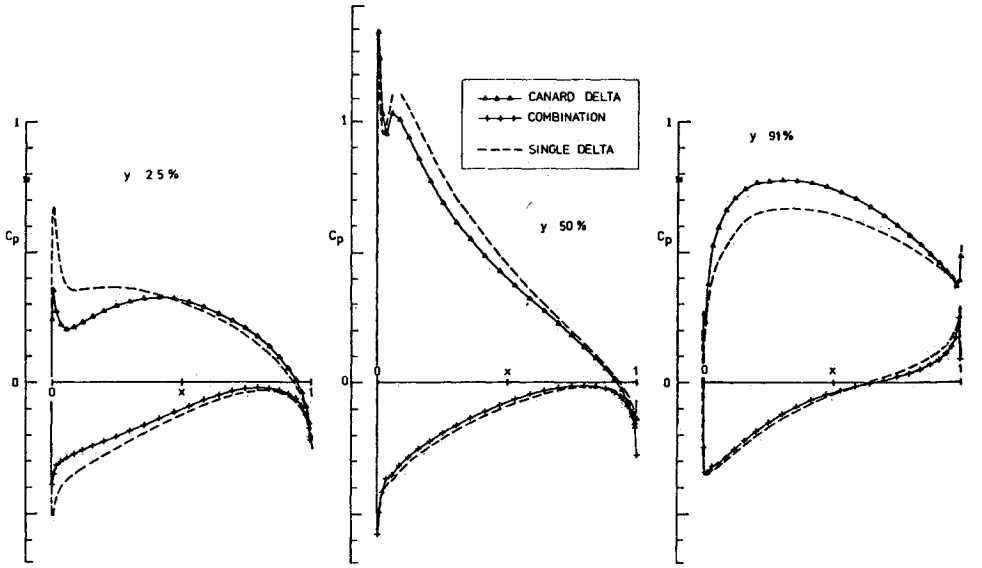

Fig 9b Influence of canard on chordwise pressure distribution (C_p vs x/c) at three sections of the main wing.

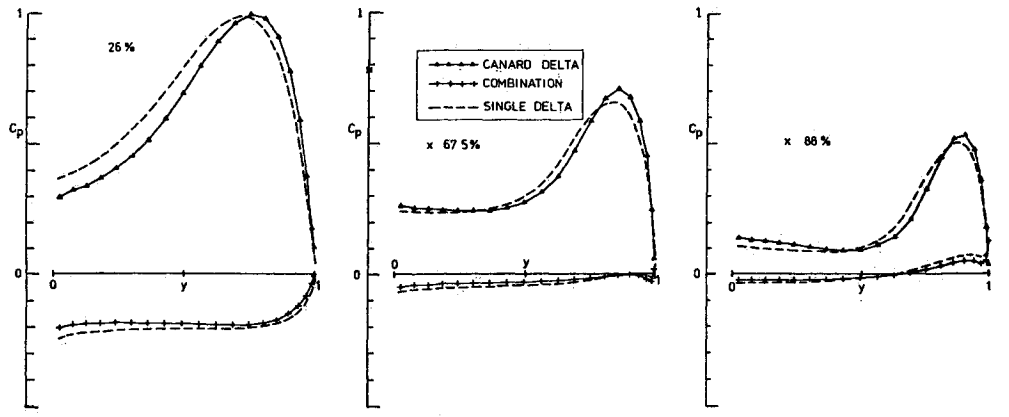

Fig 9c Influence of canard on spanwise pressure distribution (C_p vs $y/\frac{1}{2}b$) along three lines of constant x/c on the main wing.

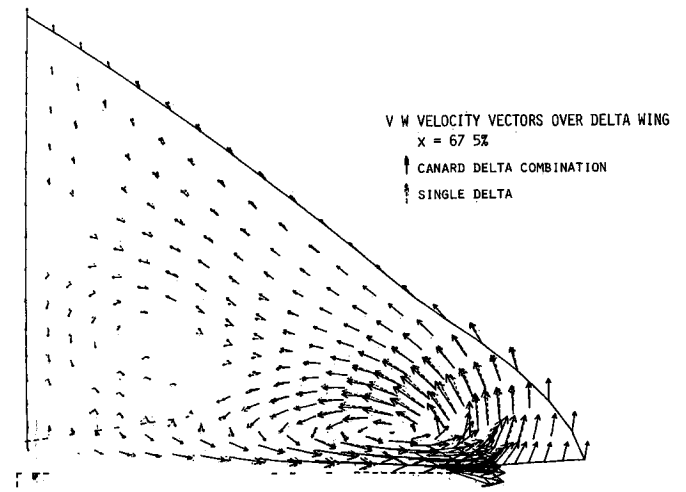

Fig. 9d Influence of canard on y z velocity components on the mesh surface that intersect the main wing along the line $x/c=67\ 5\%$ The trailing edges of the main wing and canard are indicated by dashed lines

Acknowledgment

This work has been supported in its entirety by the Air Materiel Department of the Swedish Defence Materiel Administration.

References

[1]Eriksson, L E and Rizzi A Computation of Vortex Flow Around Wings Using the Euler Equations ' *Proceedings of the 4th GAMM Conference on Numerical Methods,* edited by H Viviand Vieweg Verlag, Wiesbaden 1982 pp 87 105

[2]Rizzi, A 'Damped Euler Equation Method to Compute Transonic Flow Around Wing Body Combinations ' *AIAA Journal* Vol 20 Oct, 1982, pp 1321 1328

[3]Eriksson L E , ' A Study of Mesh Singularities and Their Effects on Numerical Errors ' FFA TN 1984 10 1984

[4]Eriksson L E Generation of Boundary Conforming Grids Around Wing Body Configurations Using Transfinite Interpolation *AIAA Journal* Vol 20 Oct 1982, pp 1313 1320

[5]Sutton, E P , Some Observations of the Flow over a Delta Winged Model with 55 deg Leading Edge Sweep at Mach Numbers between 0 4 and 1 8, ' ARC R&M 3190 1960

[6]Rizzi, A., Eriksson L E , Schmidt, W and Hitzel, S Numerical Solution of the Euler Equations Simulating Vortex Flow Around Wings ' *Aerodynamics of Vortical Type Flows in Three Dimensions* AGARD-CPP 342 Paris France 1983 pp 21 1 to 21 14.

[7] Test Cases for Steady Inviscid Transonic and Supersonic Flows,' Fluid Dynamics Panel Working Group 07 AGARD Publ in preparation 1984

[8]Hoeijmaker H W M Private communication NLR Amsterdam 1983

[9]Eriksson L E , Transfinite Mesh Generation and Computer Aided Analysis of Mesh Effects " Doctoral Thesis at Uppsala University Department of Computer Science Uppsala Sweden 1984